Synchronization in Two Polygonal Oscillatory Networks Sharing a Branch

Yoko Uwate
UZH/ETH Zurich,
Winterthurerstrasse 190,
CH-8057 Zurich, Switzerland,
Email: yu001@ini.phys.ethz.ch

Yoshifumi Nishio
Dept. of Electrical and Electronic Engineering,
Tokushima University
2-1 Minami-Josanjima, Tokushima, Japan
Email: nishio@ee.tokushima-u.ac.jp

Ruedi Stoop
UZH/ETH Zurich,
Winterthurerstrasse 190,
CH-8057 Zurich, Switzerland,
Email: ruedi@ini.phys.ethz.ch

***Abstract*—In this study, synchronization phenomena observed in two coupled polygonal oscillatory networks sharing a branch is investigated. We focus on the phase difference between two oscillators which are coupled to the shared branch of the two polygonal networks. By computer simulations, we observe that synchronization state of the shared oscillators depends on the number of coupled oscillators of the each polygonal network.**

I. Introduction

Synchronization, in particular, is one of the most important features that can be described and explored with the help of oscillators, because, upon their coupling, strongly correlated rhythms among the oscillators emerge, called synchronized states. Synchronization phenomena have been extensively reported in physical [1]-[4], biological [5],[6] and electrical [7],[8] systems.

Moreover, there are several types of polygonal network structures (e.g. Honeycomb structure and crystal structure) exists in the natural science. For the studies of large-scale network using coupled oscillators, a ring, a ladder and a two dimensional array structure are often investigated. However, there are not many discussions about coupled polygonal oscillatory networks by using electrical oscillators.

In this study, synchronization phenomena in two coupled polygonal oscillatory networks is investigated. Two polygonal oscillatory networks is shared a branch of two networks as shown in Fig. 1. First, we consider the two triangle oscillatory networks are shared by a branch. By using computer simulations and theoretical analysis, the phase difference and the amplitude of each oscillator are discussed. Furthermore, we investigate the phase difference between the shared oscillators when two polygonal (quadrilateral, pentagon, hexagon and heptagon) oscillatory networks are coupled.

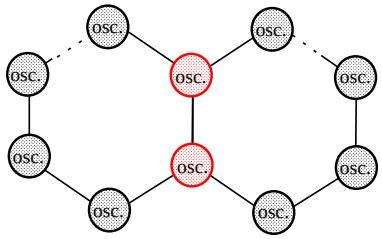

Fig. 1. General two coupled polygonal network oscillators.

II. Two Coupled Triangle Oscillatory Networks

We consider the two coupled triangle oscillatory networks sharing a branch as a first circuit model.

A. Circuit Model

The circuit model of two coupled triangle oscillatory networks sharing the branch is shown in Fig. 2.

We assume that the $v_k - i_{Rk}$ characteristics of the nonlinear resistor in each oscillator is given by the following third order polynomial equation,

$$i_{Rk} = -g_1 v_k + g_3 {v_k}^3 \quad (g_1, g_3 > 0), \qquad (k = 1, 2, 3, 4). \tag{1}$$

The normalized circuit equations governing the circuit in Fig. 2 are expressed as
[First oscillator]

$$\begin{cases} \dfrac{dx_1}{d\tau} = \varepsilon\Big(1 - \dfrac{1}{3}{x_1}^2\Big)x_1 - (y_{a1} + y_{b1} + y_{c1}) \\ \dfrac{dy_{a1}}{d\tau} = \dfrac{1}{3}\Big\{x_1 - \eta y_{a1} - \gamma(y_{a1} + y_{b2})\Big\} \\ \dfrac{dy_{b1}}{d\tau} = \dfrac{1}{3}\Big\{x_1 - \eta y_{b1} - \gamma(y_{a3} + y_{b1})\Big\} \\ \dfrac{dy_{c1}}{d\tau} = \dfrac{1}{3}\Big\{x_1 - \eta y_{c1} - \gamma(y_{b4} + y_{c1})\Big\} \end{cases} \tag{2}$$

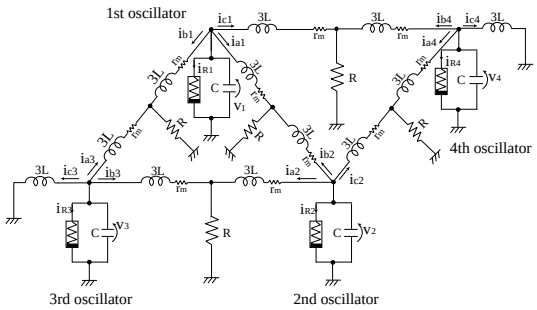

(a) Two coupled triangle oscillatory networks.

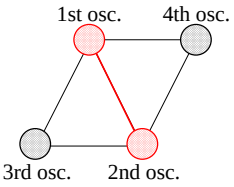

(b) Conceptual circuit model.

Fig. 2. Circuit model.

[Second oscillator]

$$\begin{cases} \dfrac{dx_2}{d\tau} = \varepsilon\left(1-\dfrac{1}{3}{x_2}^2\right)x_2 - (y_{a2}+y_{b2}+y_{c2}) \\ \dfrac{dy_{a2}}{d\tau} = \dfrac{1}{3}\left\{x_2 - \eta y_{a2} - \gamma(y_{a2}+y_{b3})\right\} \\ \dfrac{dy_{b2}}{d\tau} = \dfrac{1}{3}\left\{x_2 - \eta y_{b2} - \beta\gamma(y_{a1}+y_{b2})\right\} \\ \dfrac{dy_{c2}}{d\tau} = \dfrac{1}{3}\left\{x_2 - \eta y_{c2} - \beta\gamma(y_{a4}+y_{c2})\right\} \end{cases} \quad (3)$$

[Third oscillator]

$$\begin{cases} \dfrac{dx_3}{d\tau} = \varepsilon\left(1-\dfrac{1}{3}{x_3}^2\right)x_3 - (y_{a3}+y_{b3}+y_{c3}) \\ \dfrac{dy_{a3}}{d\tau} = \dfrac{1}{3}\left\{x_3 - \eta y_{a3} - \gamma(y_{a3}+y_{b1})\right\} \\ \dfrac{dy_{b3}}{d\tau} = \dfrac{1}{3}\left\{x_3 - \eta y_{b3} - \gamma(y_{a2}+y_{b3})\right\} \\ \dfrac{dy_{c3}}{d\tau} = \dfrac{1}{3}\left\{x_3 - \eta y_{c3}\right\} \end{cases} \quad (4)$$

[Fourth oscillator]

$$\begin{cases} \dfrac{dx_4}{d\tau} = \varepsilon\left(1-\dfrac{1}{3}{x_3}^2\right)x_3 - (y_{a4}+y_{b4}+y_{c4}) \\ \dfrac{dy_{a4}}{d\tau} = \dfrac{1}{3}\left\{x_4 - \eta y_{a4} - \gamma(y_{a4}+y_{c2})\right\} \\ \dfrac{dy_{b4}}{d\tau} = \dfrac{1}{3}\left\{x_4 - \eta y_{b4} - \gamma(y_{b4}+y_{c1})\right\} \\ \dfrac{dy_{c4}}{d\tau} = \dfrac{1}{3}\left\{x_4 - \eta y_{c4}\right\} \end{cases} \quad (5)$$

where

$$t = \sqrt{LC}\tau, \quad v_k = \sqrt{\frac{g_1}{3g_3}}x_k,$$

$$i_{ak} = \sqrt{\frac{g_1}{3g_3}}\sqrt{\frac{C}{L}}y_{ak}, \quad i_{bk} = \sqrt{\frac{g_1}{3g_3}}\sqrt{\frac{C}{L}}y_{bk},$$

$$\varepsilon = g_1\sqrt{\frac{L}{C}}, \quad \gamma = R\sqrt{\frac{C}{L}}, \quad \eta = r_m\sqrt{\frac{C}{L}},$$

$$(k = 1, 2, 3, 4).$$

In this equations, γ is the coupling strength and ε denotes the nonlinearity of the oscillators.

B. Synchronization Phenomena

For the computer simulations, we calculates Eqs. (2)-(5) using a fourth-order Runge-Kutta method with the step size $h = 0.005$. The parameters of this circuit model are fixed as $\varepsilon = 0.1$, $\gamma = 0.1$, $\eta = 0.0001$.

Figure 3 shows the time wave form of the voltage charged at the capacitance of each oscillator. From this figure, we can see that the first and the second oscillators are synchronized at in-phase (phase difference: 0 degree). While, the other combination oscillators synchronize with anti-phase (phase difference: 180 degree). Furthermore, the amplitude of between the first/second and the third/fourth oscillators has small difference. The phase plane of each combination oscillator is shown in Fig. 4.

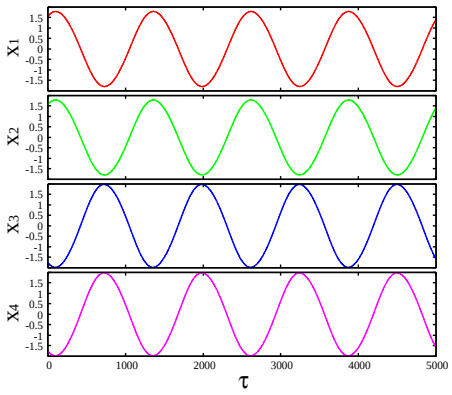

Fig. 3. Time wave form of the voltage charged at the capacitance of each oscillator.

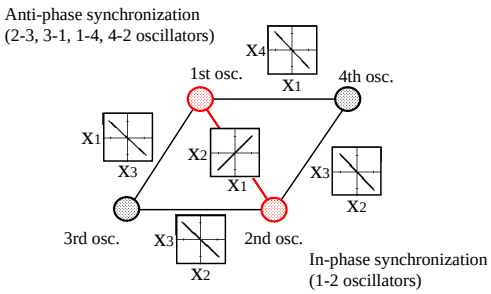

Fig. 4. Phase plane of each oscillator.

C. Theoretical Analysis

In this section, we explain the theoretical analysis by using the averaging method for the circuit equations (2)-(5) obtained from Fig. 2. Here, we consider the case of that the tiny resistance r_m does not exist ($\eta = 0$).

First, Eq (2) can be described by second order nonlinear differential equation as follows.

$$\frac{d^2x_1}{d\tau^2} + x_1 = \varepsilon(1 - {x_1}^2)\frac{dx_1}{d\tau} + \frac{1}{3}\gamma Y_1 \equiv F_1 \tag{6}$$

$$\frac{dY_1}{d\tau} + \frac{2}{3}\gamma Y_1 = x_1 + \frac{1}{3}x_2 + \frac{1}{3}x_3 + \frac{1}{3}x_4 \tag{7}$$

where,

$$Y_1 \equiv y_{a1} + y_{a3} + y_{b1} + y_{b2} + y_{b4} + y_{c1}.$$

Equation (7) is the first order linear differential equation. The solution is given as following equation.

$$\begin{aligned} Y_1 = \;& e^{-\frac{2}{3}\gamma\tau}\int e^{\frac{2}{3}\gamma\tau}\Big(x_1 + \tfrac{1}{3}x_2 + \tfrac{1}{3}x_3 + \tfrac{1}{3}x_4\Big) \\ & + Ce^{-\frac{2}{3}\gamma\tau} \\ & (C : const.) \end{aligned} \tag{8}$$

In the steady state, the second term of Eq. (8) becomes to zero.

Next, let assume the solution of Eq. (6) is

$$x_k(\tau) = \rho_k sin(\tau + \theta_k). \tag{9}$$

We pay attention to treat the non-resonance system and apply for the averaging method to Eq. (6). We obtain ρ_1 and θ_1 as follows.

$$\begin{aligned} \dot{\rho_1} &= \lim_{T\to\infty}\int_0^T \varepsilon F_1 cos(\tau + \theta_1)d\tau \\ \dot{\theta_1} &= \lim_{T\to\infty}\int_0^T \frac{\varepsilon}{\rho_1}F_1 sin(\tau + \theta_k)d\tau \end{aligned} \tag{10}$$

By solving the above equations, Eqs. (11) and (12) are obtained.

$$\begin{aligned} \dot{\rho_1} \;=\; & -\frac{\varepsilon^2\rho_k}{8}(\rho_k^2 - 4) \\ & -\frac{\varepsilon\gamma}{3(4\gamma^2+9)}\Big\{9\rho_1 + 2\gamma\rho_2 sin(\theta_1 - \theta_2) \\ & -3\rho_2 cos(\theta_1 - \theta_2) + 2\gamma\rho_3 sin(\theta_1 - \theta_3) \\ & -3\rho_3 cos(\theta_1 - \theta_3) + 2\gamma\rho_4 sin(\theta_1 - \theta_4) \\ & -3\rho_4 cos(\theta_1 - \theta_4)\Big\} \end{aligned} \tag{11}$$

$$\begin{aligned} \dot{\theta_1} \;=\; & -\frac{\varepsilon\gamma}{3\rho_k(4\gamma^2+9)}\Big\{6\gamma\rho_1 + 2\gamma\rho_2 cos(\theta_1 - \theta_2) \\ & -3\rho_2 sin(\theta_1 - \theta_2) + 2\gamma\rho_3 cos(\theta_1 - \theta_3) \\ & -3\rho_3 sin(\theta_1 - \theta_3) + 2\gamma\rho_4 cos(\theta_1 - \theta_4) \\ & -3\rho_4 sin(\theta_1 - \theta_4)\Big\} \end{aligned} \tag{12}$$

We also apply the averaging method to Eqs. (3)-(5) as similarity.

In the steady state,

$$\dot{\rho_k} = 0 \qquad and \qquad \dot{\theta_k} = 0 \qquad (k = 1, 2, 3, 4). \tag{13}$$

must be satisfied. We obtain the solutions as follows. For the amplitude:

$$\rho_k = \sqrt{4 - \frac{8\gamma}{3\varepsilon(4\gamma^2+9)}} \qquad (k = 1, 2). \tag{14}$$

$$\rho_k = 2 \qquad (k = 3, 4). \tag{15}$$

For the phase difference:

$$\theta_1 - \theta_2 = 0. \tag{16}$$

$$\theta_3 - \theta_2 = \theta_3 - \theta_4 = \theta_4 - \theta_1 = \theta_4 - \theta_2 = \pi. \tag{17}$$

We confirm that the first and the second oscillators are synchronized at in-phase. Other combination oscillators synchronize with anti-phase. These theoretical results correspond with the computer simulation results. Table I summarizes the comparison between theoretical and simulation results when the parameters are set as $\varepsilon = 0.1$! \$ $\gamma = 0.1$. From this table, we can see that they match very well.

TABLE I
COMPARISON BETWEEN THEORETICAL AND SIMULATION RESULTS FOR THE AMPLITUDE.

	Theory	Simulation
ρ_1, ρ_2	1.765	1.790
ρ_3, ρ_4	2.000	1.979

D. Case for polygonal network ($N \geqq 6$)

Finally, we investigate synchronization phenomena in several types of two coupled polygonal oscillatory networks as shown in Fig. 5. The computer simulation result of the phase difference between the shared oscillators of each network structure are summarized in Tab. II. From this table, we can see that the shared (the first and the second) oscillators are synchronized at anti-phase state when the number of the coupled oscillators of each polygonal network is even number. While in the case of that the number of the coupled oscillators of each polygonal network is odd number, the shared oscillators can not synchronized at anti-phase state.

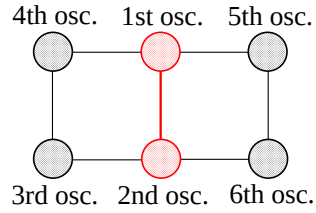

(a) quadrilateral network (N=6).

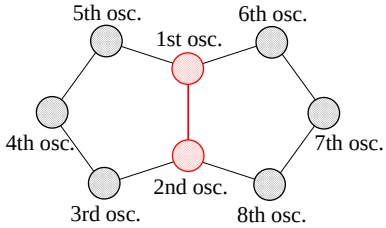

(b) pentagon network (N=8).

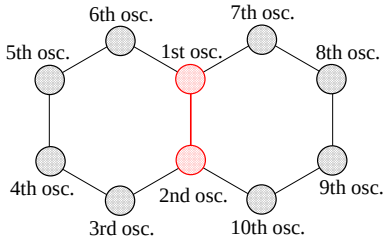

(c) hexagon network (N=10).

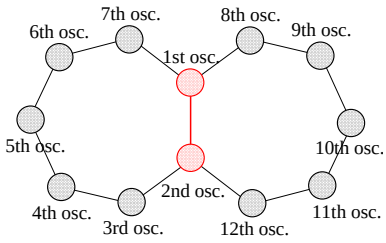

(d) heptagon network (N=12).

Fig. 5. Several types of two coupled polygonal oscillatory networks.

TABLE II
SYNCHRONIZATION STATES FOR DIFFERENT TYPES OF POLYGONAL OSCILLATORY NETWORKS

Number of oscillators	Oscillator type	Phase
N=6 (quadrilateral)	Shared osc. (1-2)	180° (anti-phase)
	Independent osc.	180° (anti-phase)
N=8 (pentagon)	Shared osc. (1-2)	107.2°
	Independent osc.	152.8°
N=10 (hexagon)	Shared osc. (1-2)	180° (anti-phase)
	Independent osc.	180° (anti-phase)
N=12 (heptagon)	Shared osc. (1-2)	128.5°
	Independent osc.	158.7°

III. CONCLUSION

In this study, we investigated synchronization phenomena in two coupled polygonal oscillatory networks sharing the branch. By computer simulations, we confirmed that synchronization state of the shared oscillators depends on the number of coupled oscillators of the each polygonal network. We assume that the shared oscillators synchronize to make balance for whole system. In order to make clear the mechanism of such synchronization, to discuss a power consumption of coupled resistor and to analyze the stability of solutions obtained from the averaging method in detail are our future works.

REFERENCES

[1] L.L. Bonilla, C.J. Perez Vicente and R. Spigler, "Time-periodic phases in populations of nonlinearly coupled oscillators with bimodal frequency distributions," *Physica D: Nonlinear Phenomena*, vol.113, no.1, pp.79-97, Feb. 1998.

[2] J.A. Sherratt, "Invading wave fronts and their oscillatory wakes are linked by a modulated traveling phase resetting wave," *Physica D: Nonlinear Phenomena*, vol.117, no.1-4, pp.145-166, June 1998.

[3] G. Abramson, V.M. Kenkre and A.R. Bishop, "Analytic solutions for nonlinear waves in coupled reacting systems," *Physica A: Statistical Mechanics and its Applications*, vol.305, no.3-4, pp.427-436, Mar. 2002.

[4] I. Belykh, M. Hasler, M. Lauret and H. Nijmeijer, "Synchronization and graph topology," *Int. J. Bifurcation and Chaos*, vol.15, no.11, pp.3423-3433, Nov. 2005.

[5] C.M. Gray, "Synchronous oscillations in neural systems: mechanisms and functions," *J. Computational Neuroscience*, vol.1, pp.11-38, 1994.

[6] R. Stoop and C. Wagner, "Neocortex's architecture optimizes computation, information transfer and synchronizability, at given total connection length," *International Journal of Bifurcation and Chaos*, vol.17, no.7, pp.2257-2279, 2007.

[7] T. Suezaki and S. Mori, "Mutual synchronization of two oscillators," *Trans. IECE*, vol.48, no.9, pp.1551-1557, Sep. 1965.

[8] H.B. Fotsina and J. Daafouza, "Adaptive synchronization of uncertain chaotic colpitts oscillators based on parameter identification" *Physics Letters A*, vol.339, pp.304-315, May. 2005.